Alginate-Polymer-Caged, C_{18}-Functionalized Magnetic Titanate Nanotubes for Fast and Efficient Extraction of Phthalate Esters from Water Samples with Complex Matrix

Hongyun Niu, Shengxiao Zhang, Xiaole Zhang, and Yaqi Cai*

State Key Laboratory of Environmental Chemistry and Ecotoxicology, Research Center for Eco-Environmental Science, Chinese Academy of Sciences, Beijing, China 100085

ABSTRACT The magnetic titanate nanotube (Fe_3O_4—TN composite) was prepared and functionalized with C_{18} groups and then coated by a hydrophilic alginate polymer cage. This material (ALG@C_{18}—Fe_3O_4—TN) exhibited the properties of large surface area, superparamagnetism, high adsorption ability, and good dispersibility in water. ALG@C_{18}—Fe_3O_4-TNs possessed high extraction efficiency to phthalate esters di-*n*-propyl-phthalate (DPP), di-*n*-butyl-phthalate (DBP), dicyclohexyl-phthalate (DCP), and di-*n*-octyl-phthalate (DOP). The dispersed adsorbents in solution could be collected with an external magnetic field within 10 min. The extraction could be conducted under some extreme conditions such as high salinity, acid or alkali solution or humic acid-rich samples without the decrease in extraction efficiency. In the presence of 100 mg L^{-1} humic acid (HAs), the recoveries of analytes were not affected at pH >6, and decreased recoveries of DPP and DCP were observed only in acid solution. Potential analysis and comparison study with the biphthalate acid or *n*-decanoic acid-rich matrix indicated that the anti-interference ability of adsorbents to HAs mainly resulted from the repulsion interaction and size exclusion provided by alginate cage to HAs. Under the optimized conditions, ALG@C_{18}—Fe_3O_4—TNs were used to analyze several environmental water samples, a concentration factor of 1000 and detection limits of phthalate esters ranging in 11—46 ng L^{-1} were achieved, and the recoveries of analytes were in the range of 84—109% for all samples.

KEYWORDS: Fe_3O_4—titanate nanotube composite • alginate polymer cage • humic acid • phthalate esters • environmental water samples

1. INTRODUCTION

Titanate nanotube (TNs), produced by the alkali hydrothermal treatment, is an intensively studied material characterized by a mesopore-range internal diameter, large surface areas and unique combination of physicochemical properties (1, 2). TNs demonstrate high ion-exchange reactivity toward alkali metal (3), transition metal (4—7), or noble metal cations (8, 9). The exchanged cations can nucleate and grow on the internal and external surface of TNs with even distribution and high dispersion to form monodispersed metallic nanocrystals during the following alkali treatment (such as ruthenium (1), gold, silver, and platinum 8, 9) or heat treatment under H_2/N_2 or N_2 flow (such as Ni and Zn 4, 5). This architecture design should be ideal for the metal nanoparticles to exhibit high reactivity and enhanced catalytic efficiency, surface plasmon absorption, or nonlinear optical properties (9). Therefore, general interest for metal doping of TNs is enormous. Among the metallic nanoparticle—TN composites, magnetic TNs have drawn the attention of researchers recently because of their possible application as semiconductors (2). Ferromagnetic or superparamagnetic Ni—, Co—, CuO—, or Fe_2O_3—TN composites have been generated by treating newly formed TNs with the corresponding metal salts in aqueous alkali solutions or using metal-doped TiO_2 powder as the starting material followed with alkali hydrothermal treatment (4, 6, 7, 10, 11). However, so far there has been no report about the successful synthesis of Fe_3O_4—TN composites.

In the present study, we have prepared Fe_3O_4—TN composites using a simple method. This material possesses large surface area and shows the characteristic of superparamagnetism. Different from other researchers, we focus on the application potential of the magnetic TNs as solid-phase extraction (SPE) adsorbents to preconcentrate organic pollutant. In our previous study, we reported that ionic surfactant (CTAB) modified TNs packed in a column can extract efficiently trace level of organic contaminants from environmental samples (12). However, the nanoscaled size of TNs leads to the high back-pressure of cartridges or columns and decreases the loading rate of water samples. The TN-packed SPE column are then impractical for large-scale water treatment (13).

Recently, magnetic materials and magnetic separation technique have gained great attention in the field of environmental purification, which produce no contaminants such as flocculants and have the capability of treating large amount of wastewater within a short time (14). On the basis

* Corresponding author. E-mail: caiyaqi@rcees.ac.cn. Tel: (086) 010-62849239. Fax: (086) 010-62849182.
Received for review January 5, 2010 and accepted March 4, 2010

DOI: 10.1021/am100010x

of this technique, we have developed a novel SPE method using magnetic nanoparticles (15). The magnetic property of Fe_3O_4—TNs makes it possible to use our synthesized material as SPE adsorbents with this method to pretreat large volume of water sample quickly. To enhance the adsorption ability of organic pollutants on the Fe_3O_4—TN surface, we functionalized this material with C_{18} groups using the silylation reaction (16, 17), which is the most commonly used method to modify metal surfaces through reaction with hydroxyl groups on the surface oxide film (18). However, the C_{18}-modified Fe_3O_4—TNs (C_{18}—Fe_3O_4—TN) display poor dispersion in water solution, probably because of their high hydrophobicity and small size. To solve this problem, we encapsulated the hydrophobic adsorbents into a cross-linked alginate polymer to avoid the direct contact of C_{18} groups with water. Alginate (ALG) is a natural anionic polysaccharide and a linear binary copolymer (19). By association with most divalent cations, ALG can produce thermally irreversible polymers (20). In the environmental field, ALG has been used to cage activated carbon or carbon nanotubes to form beads to remove heavy metal ions or organic dyes from polluted water (13, 14, 19, 20). The polymer cage is reported to have selective permeation properties and provide desirable protection of adsorptive sites from being damaged by adsorbing chemical of large molecular weight (such as humic acid or colloids) because of the electrostatic repulsion or size exclusion effect (13). It can be expected that the alginate caged C_{18}—Fe_3O_4—TNs (ALG@C_{18}—Fe_3O_4—TNs) exhibit great advantage over commercial SPE adsorbents in pretreating large volumes of environmental water samples for their large surface areas, superparamagnetism, highly hydrophobic surface, and anti-interference ability to a complex matrix.

2. EXPERIMENTAL SECTION

2.1. Chemicals and Materials. Sodium alginate was of chemical pure (Xilong Chemical Factory, Shantou, Guangdong Province) and purified in acetonitrile solvent with ultrasonication for three times before use. Ferric chloride ($FeCl_2 \cdot 4H_2O$), ferrous chloride ($FeCl_3 \cdot 6H_2O$), barium chloride ($BaCl_2 \cdot 2H_2O$), and sodium hydroxide (NaOH) were of analytical reagent grade and purchased from Beijing Chemicals Corporation (Beijing, China), and used without further purification. Di-*n*-propyl-phthalate (DPP), di-*n*-butyl-phthalate (DBP), dicyclohexyl-phthalate (DCP), and di-*n*-octyl-phthalate (DOP) were obtained from Acros Organics (New Jersey). Octadecyltriethoxysilane (ODS) was supplied by Tokyo Chemical Industry Co. Ltd. (Tokyo). Ultrapure water was prepared using the Milli-Q water purification system (Millipore, Bedford, MA).

2.2. Synthesis of ALG@C_{18}—Fe_3O_4—TN Magnetic Nanomaterials. Protonated TNs were prepared with hydrothermal method described in ref 12. To produce the composited Fe_3O_4—TN magnetic adsorbents, 0.5 g of TNs was dispersed in 200 mL of deoxygenated water containing 0.22 g $FeCl_2 \cdot 4H_2O$ and 0.60 g $FeCl_3 \cdot 6H_2O$ in a conical flask. The mixed suspension was stirred vigorously for 3 h under N_2 protection at 353 K, and the color of the mixture was changed from white to orange after equilibrium. Then, 0.5 M NaOH solution was added dropwise into this mixture under stirring, ultrasonication, and nitrogen gas protection to introduce Fe_3O_4 nanoparticles onto TNs based on the coprecipitation method (15, 21). The final pH of solution was about pH 11.0. The obtained magnetic nanomaterials were black in color, and the mass ratio of TNs/Fe_3O_4 was about 2:1.

The synthesized Fe_3O_4—TN composites were rinsed with 100 mL of ethanol, subsequently with 20 mL of anhydrous toluene twice, dispersed into 80 mL of anhydrous toluene, and then ultrasonicated for 5 min with the addition of 1 mL of ODS. The mixtures were transferred into a PTFE-lined autoclave and heated at 393 K for 12 h. The obtained Fe_3O_4—C_{18} nanoparticles were washed with toluene, acetone, ethanol containing 50% 0.1 M HCl aqueous solution, and absolute ethanol subsequently.

The as-prepared C_{18}—Fe_3O_4—TN nanomaterials were dispersed into 200 mL of sodium alginate solution (0.2%), and then 40 mL of 0.1 M barium chloride solution was dropped into the mixture under ultrasonication and vigorous stirring. After being aged for 30 min, the obtained adsorbents were separated from solution by a powerful magnet and washed with DI water to remove the redundant barium ions. The resulted barium alginate caged Fe_3O_4—C_{18} adsorbent (ALG@C_{18}—Fe_3O_4—TNs) were freeze-dried for use. Illustration of the preparation procedure is shown in Figure 1 a.

The images of nanomaterials in different stages were recorded by transmission electron micrograph (TEM) and scanning electron micrograph (SEM). The crystalline and surface chemistry property of the adsorbents was characterized by X-ray powder diffractometer and Nicolet Avatar 360 spectrometer, respectively. Magnetic property of the adsorbents was analyzed using a vibrating sample magnetometer (VSM, LDJ9600). The specific surface areas of adsorbents were determined by the BET method with N_2 gas. The detailed information was shown in the Supporting Information.

2.3. SPE Procedure. ALG@C_{18}—Fe_3O_4—TNs was used as SPE adsorbents to preconcentrate several phthalate esters from water samples according to the procedure described in ref 15. As shown in Figure 1b, a suitable amount of ALG@C_{18}—Fe_3O_4—TN adsorbents were rinsed and activated with 5 mL of methanol, and then dispersed into a 500 mL water sample. The mixture was stirred with a glass rod for 1 min and placed for a certain time. Subsequently, an Nd—Fe—B strong magnet ($150 \times 130 \times 50$ mm^3) was deposited at the bottom of the beaker and the adsorbent were isolated from the solution. After about 10 min, the solution became transparent and the liquid phase was discarded. Finally, the preconcentrated target analytes were eluted from the isolated adsorbents with acetonitrile. The eluent was concentrated with a stream of nitrogen at 50 °C and reconstituted in 0.5 mL of acetonitrile. Twenty-microliter aliquots were injected into the HPLC system for analysis. HPLC conditions for phthalate esters analysis are listed in the Supporting Information.

3. RESULTS AND DISCUSSION

3.1. Loading of Fe_3O_4 in/onto TNs. In a typical ion-exchange method, a final aqueous washing step is applied before alkali treatment in order to eliminate excess unexchanged ions. However, in our study, we found that it was necessary to maintain an excess amount of ferric and ferrous ions in mixture after equilibrium to produce Fe_3O_4—TN composites. If these cations were removed after equilibrium by filtration or centrifugation, the color of the solid would remain unchanged (orange) with the following alkali treatment. Though nanoparticles with dimensions of 2—6 nm confined in the hollow cavity or supported on the surface of TNs were observed in TEM images (see Figure S1a in the Supporting Information), the products showed weak magnetic property. The XRD patterns in Figure 2 indicated that the crystal phase of this composite was that of $H_2Ti_3O_7$ (1, 2)

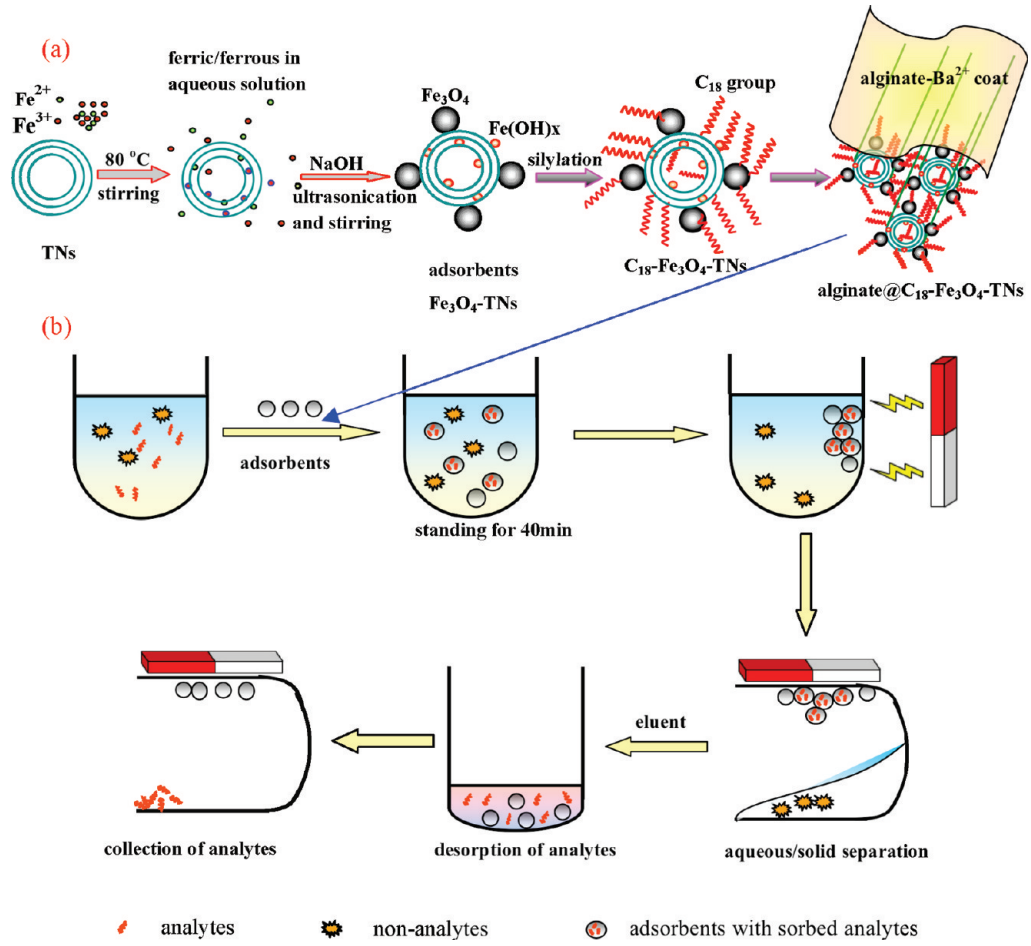

FIGURE 1. Schematic diagram of (a) the preparation of ALG@C_{18}−Fe_3O_4−TN adsorbent, and (b) its application for enriching analytes as SPE sorbents.

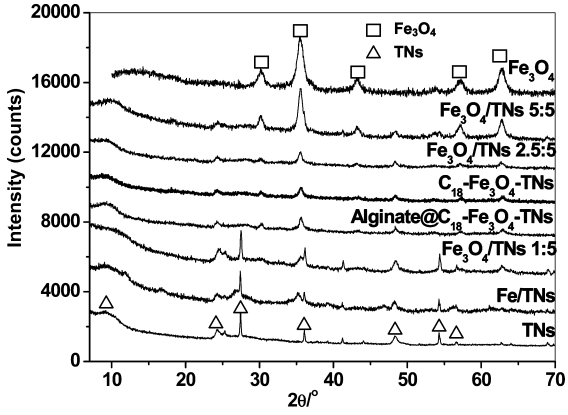

FIGURE 2. XRD patterns of Fe_3O_4 nanoparticles and Fe_3O_4−TN, TN, Fe_3O_4−TN composites with different Fe_3O_4/TN ratios, C_{18}−Fe_3O_4−TN, and ALG@C_{18}−Fe_3O_4−TNs.

and Fe_2O_3 (22), and the diffraction peaks for FeO (23) or Fe_3O_4 were hardly detected. The absence of FeO peaks might result from the low loading of ferrous oxide prepared with ion-exchange method. Because the Fe(III) and Fe(II) ions were intercalated into the crystalline of TNs separately and occupied different positions on the TN surface, it was probably hard to form Fe_3O_4 particles, which are a composite of Fe(III) oxide and Fe(II) oxide. On the other hand, the exchange of protons with Fe^{3+}/Fe^{2+} ions was also essential to ensure the firmly bonding of Fe_3O_4 nanoparticles on the surface of TNs. If the ferric/ferrous ions were added into alkali TNs solution directly, the majority of produced Fe_3O_4 nanoparticles (with an average diameter of 10 nm) were isolated from TNs and aggregated seriously (see Figure S1b in the Supporting Information).

To obtain the optimal Fe_3O_4−TN composites, we ranged the mass ratio of the theoretical Fe_3O_4/TNs in reaction solution from 0.2 to 1.0 (the product coded as $Fe_3O_4(x)$ x = 0.2, 0.4, 0.5 0.6, and 1.0). The results showed that the color of these products was changed from fulvous to black with the increase in the amount of Fe_3O_4 in the composite. The typical TEM images of Fe_3O_4−TN composites are shown in Figure 3. There were also a few small particles (2−6 nm) in the inner space or outer surface of nanotubes, whereas a large number of quasi-spherical-shaped, monodispersed nanoparticles were distributed on the outer surface of TNs, and their diameters were about 10−20 nm (Figure 3a, b). The bonding interaction between the surface atoms of these nanoparticles and the surrounding oxygen atoms of the TNs was so strong that all these particles could be stably kept on the TN surface under ultrasonication, vigorous stirring, or heat. In XRD patterns, Bragg reflections for the composites could be indexed to the mixture of $H_2Ti_3O_7$ and cubic crystalline bulk magnetite (Fe_3O_4) (Figure 2). The intensity of Fe_3O_4 peaks and the saturation magnetization of the

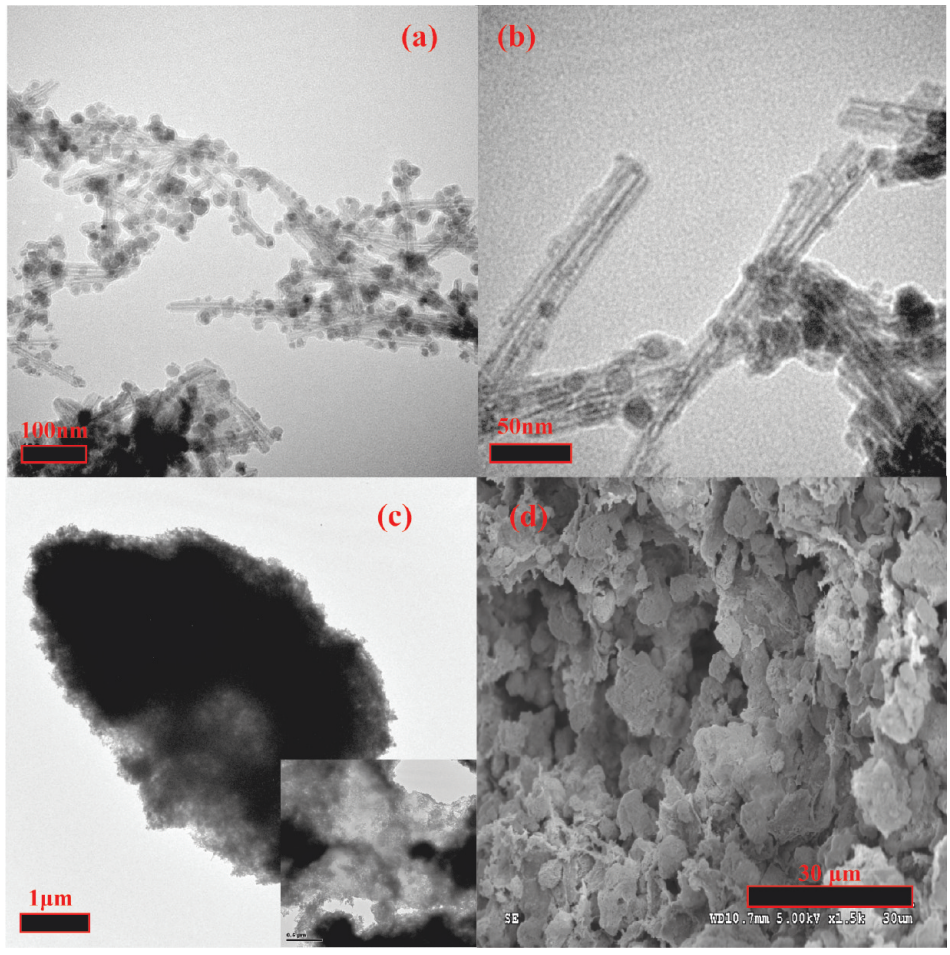

FIGURE 3. (a, b)TEM image of Fe_3O_4−TNs, (c) TEM and (d) SEM image of ALG@C_{18}−Fe_3O_4−TNs.

composites increased with the increase in Fe^{3+}/Fe^{2+} amount in reaction solution, for example, the saturation magnetization was 8, 11, and 19 emu g^{-1} for Fe_3O_4 (0.4), Fe_3O_4 (0.5), and Fe_3O_4 (0.6), respectively (see Table S1 in the Supporting Information). But the enhanced iron proportion gave rise to the increased average particle diameters of the bonded Fe_3O_4 particles. When the ratio of Fe_3O_4/TNs was higher than 0.5, Fe_3O_4 diameters increased to 30−50 nm, and nanoparticles isolated from TNs were also observed (see Figure S1c,d in the Supporting Information). This phenomenon was consistent with the magnetism properties of these composites. In the VSM magnetization curves of Fe_3O_4 (0.4) and Fe_3O_4 (0.5) obtained at room temperature, there was no hysteresis, and the remanence and coercivity was negligible, indicating the superparamagnetism and nanoscaled size of the two materials (see Figure S2 and Table S1 in the Supporting Information). For Fe_3O_4 (0.6), clear hysteresis was observed, and the remanence and coercivity were 3.97 emu g^{-1} and 54 Oe, respectively, which reflected the ferromagnetic characteristic and large size of this adsorbent.

The specific surface area (SSA) of Fe_3O_4−TN composites decreased obviously compared with the initial TNs (313 m^2 g^{-1}), and the SSAs for Fe_3O_4 (0.2)−Fe_3O_4 (1.0) were 223, 197, 190, 187, and 163 m^2 g^{-1}, respectively. Considering the saturation magnetization, surface areas, and integrity of structure of the composite, Fe_3O_4 (0.5) was regarded as the desired adsorbent.

3.2. Characteristic of the Biotin-Coated C_{18}−Fe_3O_4−TN Adsorbents. The SEM and TEM images of ALG@C_{18}−Fe_3O_4-TNs are shown in Figure 3c, d. The adsorbents prepared in our study were of block structure instead of the spherical shape of activated carbon− or carbon nanotube−alginate bead (13, 14, 19, 20). As shown in the Figure 3c inset, there were substantive Fe_3O_4−TN composite embodied in one alginate cage. The size of the ALG@C_{18}−Fe_3O_4−TNs was larger than several micrometers (Figure 3d). In the XRD pattern, the crystalline of magnetic TNs composite was unchanged after coating with alginate polymer (Figure 2). But one-third of the saturation magnetization was decreased with the polymer coat (7.3 emu g^{-1}) (see Figure S2 and Table S1 in the Supporting Information), indicating that the coat was thick, whereas superparamagnetism of adsorbent was still maintained. In the FTIR spectrum of ALG@C_{18}−Fe_3O_4−TN, adsorption peaks for C_{18} groups, hydroxyl, and carboxylic groups of alginate polymers could be discerned clearly, demonstrating the successful immobilization of C_{18} groups on the surface of Fe_3O_4−TNs composites and coating of alginate polymer on the surface of C_{18}−Fe_3O_4−TNs (22, 24) (see the Supporting Information, Figure S3).

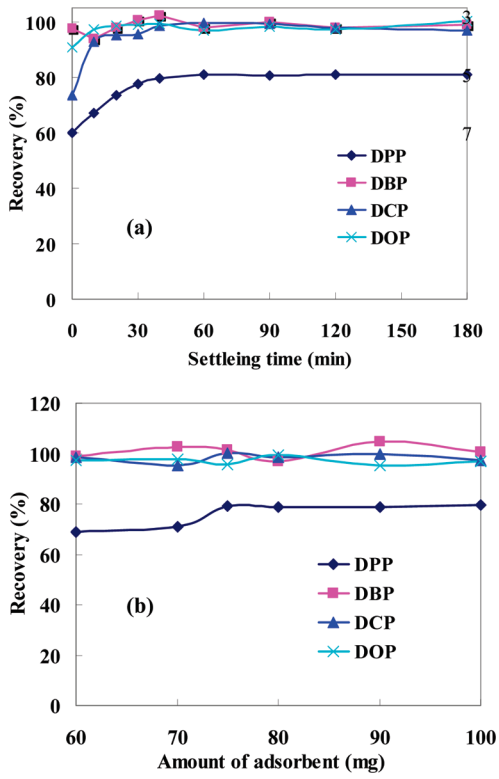

FIGURE 4. Effect of (a) setting time and (b) adsorbent amount on the SPE efficiency of phthalate esters by ALG@C_{18}−Fe_3O_4−TN.

3.3. Optimization of Extraction Conditions. The application potential of ALG@C_{18}−Fe_3O_4-TNs as SPE adsorbents was investigated by extracting a trace level (4 ng mL^{-1}) of phthalate esters from 500 mL aqueous samples. Different from the traditional SPE procedure, sufficient contact time was necessary to guarantee the adsorption equilibrium of target compounds on adsorbents. Thereby, after being stirred with a glass rod for 1 min, the mixture containing analytes and adsorbents was left to stand for a certain time (0−180 min) before phase separation. The results showed that more than 90% of DBP and DOP, 70% of DCP, and 60% of DPP were recovered from 500 mL of solution with 0 min of standing time. After contact for 10−20 min, the maximum recoveries (close to 100%) for DBP, DCP, and DOP were obtained. For DPP, the adsorption equilibrium was reached after standing for 40 min (Figure 4a). Generally, the adsorption of phthalate esters on ALG@C_{18}−Fe_3O_4−TNs was very fast.

To obtain the maximum recoveries of target analytes, the amount of the adsorbents required was optimized by varying ALG@C_{18}−Fe_3O_4−TN amount from 60 to 100 mg. As a result, the recoveries for DBP, DCP, and DOP were kept constant and near 100% in the whole range (Figure 4b). For the relatively polar DPP, the recovery was enhanced from 65 to 80% as the ALG@C_{18}−Fe_3O_4−TN amount increased to 75 mg, and was then unchanged with the further increase in adsorbent amount. Compared with the conventional C_{18} adsorbent (250−500 mg), the required ALG@C_{18}−Fe_3O_4−TN amount was rather low to pretreat large volumes of water samples, which might be caused by its large surface area and high adsorption capacity. The adsorbed analytes could be desorbed easily from ALG@C_{18}−Fe_3O_4−TNs with acetonitrile. Using 3 mL of acetonitrile, we eluted 90% of each analyte adsorbed; with 6 mL of acetonitrile, the maximal recoveries for all the analytes were obtained. In the following experiments, the standing time, amount of adsorbent, and volume of eluate were 40 min, 80 mg (containing 68.6 mg of C_{18}−Fe_3O_4−TNs), and 6 mL, respectively.

3.4. Extraction Efficiency of ALG@C_{18}−Fe_3O_4−TN Adsorbents to Phthalate Esters under Some Extreme Conditions. The effect of solution pH on the recoveries of the model compounds was investigated by varying the pH from 3.0 to 10.0. The results showed that the recoveries of all these compounds kept unchanged in the whole pH range. TNs were known to be of acid and alkaline resistance; however, the Fe_3O_4 particles were readily dissolved in acid solution. The high extraction efficiency of this magnetic adsorbent at pH 3.0 might indicate its integrity, which should result from the protection provided by the coated hydrophilic alginate polymer. Therefore, compared with the widely used silica-based adsorbents, ALG@C_{18}−Fe_3O_4−TN displayed its great advantage in pretreatment special water samples with high acidity or alkalinity.

The effects of salt addition to water containing organic pollutants prior their extraction has been studies as a favoring factor because, in theory, high ionic strength improves extraction of organic compounds (24). In this study, 0−400 mM NaCl were added to the solution to examine the impact of ionic strength on the recoveries of target compounds. The results indicated that the recoveries of all the target analytes were independent of the salt concentration.

3.5. Anti-interference Ability of ALG@C_{18}−Fe_3O_4−TN Adsorbents to Humic Acid. For SPE, the negative effect of humic acids (HAs) was found when C_{18} silica was used to extract nonpolar analytes and pesticides due to the association of organic pollutant with HAs or the retention of HAs on solid-phase material (25, 26). The effect of HAs on the extraction efficiency of phthalate esters was assessed in the presence of HAs in neutral solution. Surprisingly, the recoveries of phthalate esters were unchanged as the concentration of HAs increased from 5 to 100 mg L^{-1} (see Figure S4 in the Supporting Information). In the molecules of HAs and ALG, there were many oxygen-containing functional groups such as carboxyl group and hydroxyl group. Since the charges and state of these functional groups were both pH-dependent, recoveries of analytes on ALG@C_{18}−Fe_3O_4−TN at different solution pH in the presence of 100 mg L^{-1} of HAs were also investigated. At pH 3.0, the recovery of DPP decreased to 36%, and then increased gradually until pH 6.0. A slight increase of DCP recoveries (from 89−96%) was also observed in this pH range. But the extraction efficiencies for DBP and DOP were generally not reduced across the pH 3.0−9.5, which might result from their high hydrophobicity (Figure 5a).

The ζ-potential isotherms of HAs and ALG−C_{18}−Fe_3O_4−TN at pH 3.0−10 determined in 10 mM $NaNO_3$ solution are

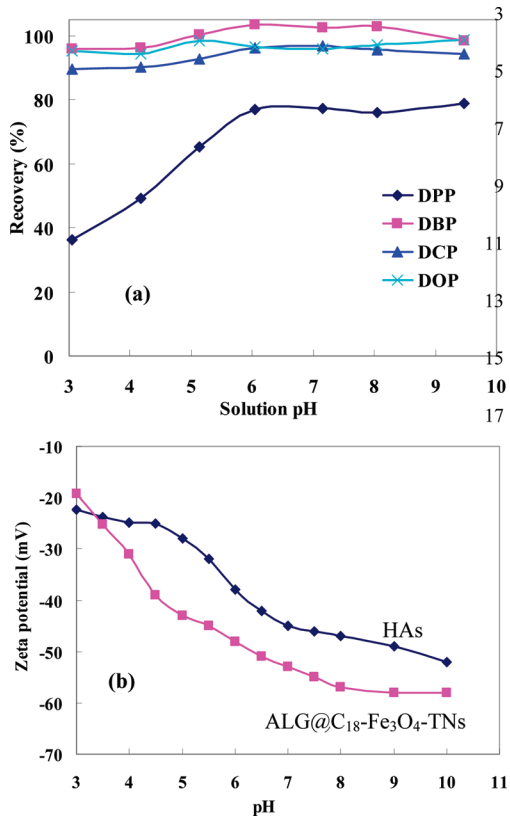

FIGURE 5. (a) Effect of solution pH on the recovery of phthalate esters in the presence of 100 mg L^{-1} HAs extracted by ALG@C_{18}−Fe_3O_4−TN and (b) ζ-potential isotherms of HAs (100 mg L^{-1}) and ALG−C18−Fe_3O_4−TNs at pH 3.0−10 in 10 mM $NaNO_3$ solution.

shown in Figure 5b. The two materials were all negatively charged even at pH 3.0 because of the ionization of carboxylic groups. Similar results had been reported by Fugetsu (13) or Lu (27). Thereby, repulsive interaction between HAs and alginate cage existed in acid solution. In the pH range of 3.0−5.0, the depronation of −COOH group in HAs was very slow, which indicated that ionization of HAs started in this pH range and the density of negative charge of HAs was low and the interaction between HAs and adsorbent should be weak. With the increase in solution pH, the ζ-potential of HAs and adsorbent decreased obviously, suggesting the increased density of negative charge of the two materials. Correspondingly, the electrostatic interactions between HAs and alginate polymer were enhanced in neutral and alkali solution. The repulsive interactions could keep HAs away from adsorbents and hard to compete the adsorptive sites with analytes (13). In Figure 5a, the antiresistance ability of adsorbent to HAs at different solution pH was consistent with the change of charge density of the two materials. This result suggested that the electrostatic repulsion to HAs provided by the negatively charged surface of alginate cage took a major role on avoiding the interference of HAs, which was consistent with the conclusion made by Fugetsu et al. (13).

In a comparison study, the SPE efficiencies of analytes in the presence of 100 mg L^{-1} of biphthalate acid (pK_{a1} = 2.89, pK_{a2} = 5.54) or *n*-decanoic acid (pK_a = 5.3, lgKow 4.2) both possessing carboxylate groups were investigated at pH 3.0 and 9.5. Similarly, the recoveries of analytes were less affected in alkaline solution except the polar analyte DPP (see Table S2 in the Supporting Information). The recovery of DPP was lower than its maximal value even at pH 9.5 in the presence of biphthalate acid and *n*-decanoic acid (68.2 and 60.8%, respectively). Furthermore, in acid solution, the recoveries of phthalate esters were lower than those in the presence of HAs. According to these results, we proposed that the electrostatic repulsion between biphthalate acid or *n*-decanoic acid and alginate cage could not completely restrict their access to inner surface of adsorbent due to the small molecular size. Although the molecular weight of naturally occurred humic acids were of 500−2000 Da (28), almost all the HAs were polydisperse in molecular weight distribution and the average molecular diameter of HAs was nearly 10-fold larger than that of common organic pollutant molecules (24). Thereby, size exclusion of alginate cage was important for the resistance of HAs. It also could be concluded that the competitive adsorption of organic acid of small molecule on ALG@C_{18}−Fe_3O_4−TNs could not reduce the extraction efficiency of organic analytes with high hydrophobicity in neutral or alkaline solution, which might result from the excellent adsorption capacity of the adsorbents.

3.6. Application of ALG@C_{18}−Fe_3O_4−TNs in Environmental Samples with Different Matrixes. Under the optimal conditions, calibration curves were established for analytes in the range of 0.06−10 ng mL^{-1}. The eluate was dried with a nitrogen flow at 333 K and the residue was redissolved into 0.5 mL acetonitrile, the preconcentration factor of 1000 was achieved for the target analytes. Quantitative parameters such as linear range, correlation coefficient, detection limit were evaluated and the results are shown in Table S3 in the Supporting Information. It could be seen that the present method had high sensitivity, wide linear range, and good precision. Each of the analyte exhibited good linearity with correlation coefficient $r^2 > 0.99$ in the studied range. The detection limits, calculated by using signal-to-noise ratio of 3, for analytes were in the range of 11−36 ng L^{-1}.

To evaluate the feasibility of the method for the analysis of phthalate esters, it was applied to determine these analytes in rainwater, tap water, wastewater, and river water samples (samples information is shown in the Supporting Information). It was turned out that DBP and DOP were detected in all the water samples, and the concentration of the two analytes in rainwater and tap water were much higher than those in surface water samples. Trace levels of DPP were found in rainwater and wastewater samples. Table S4 in the Supporting Information shows the recoveries and concentrations of the target compounds in the real water samples, expressed as mean value (n = 3), and the relative standard deviation (RSD) of recoveries ranged from 0.3 to 11. The results indicated that the recoveries of spiked solution for all the samples were very satisfactory. The recoveries of analytes ranged from 84 to 109%. Chromatograms of phthalate esters in North Moat river sample and its spiked solution are shown in Figure 6.

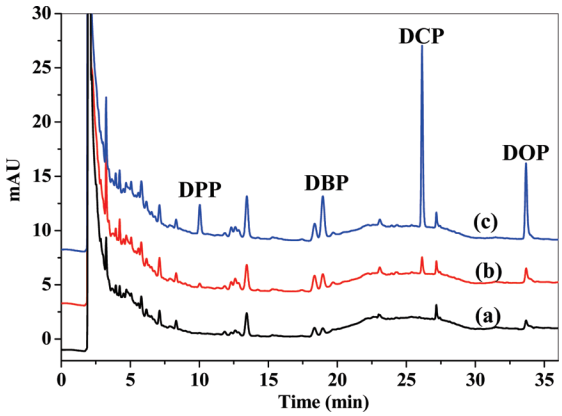

FIGURE 6. Solid-phase extraction/LC-FLD chromatograms of North Moat river samples: (a) river water sample, (b) river water spiked with 0.2 ng mL^{-1} of phthalate esters, and (c) river water spiked with 2 ng mL^{-1} phthalate esters.

CONCLUSIONS

In summary, we prepared alginate-polymer-caged magnetic titanate nanotubes for the first time with a simple method. The superparamagnetic property and magnetic SPE technique ensured that analytes in aqueous solution could be collected within a short time. The alginate polymer cage showed great anti-interference ability to humic acid-rich matrix without the decrease of extraction efficiency of analytes. The ALG@C_{18}−Fe_3O_4−TNs exhibited a great advantage over the silica-based adsorbents to pretreat large volume of water samples with complex matrix. Because of the stability, superparamagnetism, anti-interference ability, and biocompatibility of this novel adsorbent, it may have potential applications in many fields.

Acknowledgment. This work was jointly supported by National High Technology Research and Development Program of China (2009AA061603); the Major State Basic Research Development Program of China (2009CB421605); the Major Research Program of the Chinese Academy of Sciences (KZCX2-YW-420-1); and the National Natural Science Foundation of China (20890111, 20907061, 20877079).

Supporting Information Available: Four tables, four figures, and details about adsorbent characterization, HPLC analysis of phthalates esters, and water sample information (PDF). This material is available free of charge via the Internet at http://pubs.acs.org.

REFERENCES AND NOTES

(1) Bavykin, D. V.; Lapkina, A. A.; Plucinski, P. K.; Friedrich, J. M.; Walsh, F. C. *J. Catal.* **2005**, *235*, 10–17.
(2) Bavykin, D. V.; Friedrich, J. M.; Walsh, F. C. *Adv. Mater.* **2006**, *18*, 2807–2824.
(3) Ma, R. Z.; Sasaki, T.; Bando, Y. *Chem. Commun.* **2005**, 948–950.
(4) Jiang, J. H.; Gao, Q. M.; Chen, Z.; Hu, J.; Wu, C. D. *Mater. Lett.* **2006**, *60*, 3803–3808.
(5) Xu, J. C.; Lu, M.; Guo, X. Y.; Li, H. L. *J. Mol. Catal. A: Chem.* **2005**, *226*, 123–127.
(6) Huang, C.; Liu, X.; Kong, L.; Lan, W.; Su, Q.; Wang, Y. *Appl. Phys. A: Mater. Sci. Process.* **2007**, *87*, 781–786.
(7) Wu, D.; Chen, Y.; Liu, J.; Zhao, X.; Li, A.; Ming, N. *Appl. Phys. Lett.* **2005**, *87*, 112501–112503.
(8) Bavykin, D. V.; Lapkin, A. A.; Plucinski, P. K.; Murciano, L. T.; Friedrich, J. M.; Walsh, F. C. *Top. Catal.* **2006**, *39*, 151–159.
(9) Ma, R. Z.; Sasaki, T.; Bando, Y. *J. Am. Chem. Soc.* **2004**, *126*, 10382–10388.
(10) Han, W. Q.; Wen, W.; Yi, D.; Liu, Z. X.; Maye, M. M.; Lewis, L.; Hanson, J.; Gang, O. *J. Phys. Chem. C* **2007**, *111*, 14339–14342.
(11) Umek, P.; Pregelj, M.; Gloter, A.; Cevc, P.; Jagličić, Z.; Čeh, M.; Pirnat, U.; Arčon, D. *J. Phys. Chem. C* **2008**, *112*, 15311–15319.
(12) Niu, H. Y.; Cai, Y. Q.; Shi, Y. L.; Wei, F. S.; Mou, S. F.; Jiang, G. B. *J. Chromatogr. A* **2007**, *1172*, 113–120.
(13) Fugetsu, B.; Satoh, S.; Shiba, T.; Mizutani, T.; Lin, Y. B.; Terui, N.; Nodasaka, Y.; Sasa, K.; Shimizu, K.; Akasaka, T. *Environ. Sci. Technol.* **2004**, *38*, 6890–6896.
(14) Rocher, V.; Siaugue, J. M.; Cabuil, V.; Bee, A. *Water Res.* **2008**, *42*, 1290–1298.
(15) Zhao, X. L.; Shi, Y. L.; Cai, Y. Q.; Mou, S. F. *Environ. Sci. Technol.* **2008**, *42*, 1201–1206.
(16) Zhang, C. M. X.; Jiang, H.; Tian, B. L.; Wang, X. J.; Zhang, X. T.; Du, Z. L. *Eng. Aspects* **2005**, *257−258*, 521–524.
(17) Niu, H. Y.; Cai, Y. Q. *Anal. Chem.* **2009**, *81*, 9913–9920.
(18) Kuwahara, Y.; Maki, K.; Matsumura, Y.; Kamegawa, T.; Mori, K.; Yamashita, H. J. *Phys. Chem. C* **2009**, *113*, 1552–1559.
(19) Zhao, H. Y.; Zheng, W.; Meng, Z. X.; Zhou, H. M.; Xu, X. X.; Li, Z.; Zheng, Y. F. *Biosens. Bioelectron.* **2009**, *24*, 2352–2357.
(20) Park, H. G.; Kim, T. W.; Chae, M. Y.; Yoo, I. K. *Process Biochem.* **2007**, *42*, 1371–1377.
(21) Wang, Z. F.; Guo, H. S.; Yu, Y. L.; He, N. Y. *J. Magn. Magn. Mater.* **2006**, *302*, 397.
(22) Schimanke, G.; Martin, M. *Solid State Ionics* **2000**, *136−137*, 1235.
(23) Bechta, S. V.; Krushinov, E. V.; Almjashev, V. I.; Vitol, S. A.; Mezentseva, L. P.; Petrov, Yu. B.; Lopukh, D. B.; Khabensky, V. B.; Barrachin, M.; Hellmann, S.; Froment, K.; Fischer, M.; Tromm, W.; Bottomley, D.; Defoort, F.; Gusarov, V. V. *J. Nucl. Mater.* **2006**, *348*, 114–121.
(24) Štengl, V.; Bakardjieva, S.; Šubrt, J.; Večerníková, E.; Szatmary, L.; Klementová, M.; Balek, V. *Appl. Catal., B* **2006**, *63*, 20–30.
(25) Jiménez, B.; Moltó, J. C.; Font, G. *Chromatographia* **1995**, *41*, 318–314.
(26) Li, N. Q.; Lee, H. K. *Anal. Chem.* **2000**, *72*, 5272–5279.
(27) Lu, C.; Su, F. *Sep. Purif. Technol.* **2007**, *58*, 113–121.
(28) Bonifazi, P.; Pierini, E.; Bruner, F. *Chromatographia* **1997**, *44*, 595–600.

AM100010X